

Time-of-Flight Ultra-Small-Angle Neutron Scattering Instrument for the SNS

M. Agamalian^a, J.M. Carpenter^{a,b}, K.C. Littrell^b, P. Thiyagarajan^b and Ch. Rehm^a

^a Spallation Neutron Source, Oak Ridge National Laboratory, Oak Ridge, TN 37813

^b Intense Pulsed Neutron Source, Argonne National Laboratory, Argonne, IL 60439

ABSTRACT

The present calculations describing the Bonse-Hart Ultra-Small-Angle Neutron Scattering (USANS) Instrument with triple-bounce Si channel-cut crystals show that significant gains in neutron flux and Q-resolution can be achieved using multiple high-order Bragg reflections. These reflections become usable only after combining the Bonse-Hart and Time-of-Flight techniques, thus this variant of the USANS camera needs a pulsed neutron source. We clearly demonstrate that new instruments of that type installed at the SNS water moderator will improve the current state-of-the art USANS camera dramatically increasing the neutron flux and sharpening the Q-resolution by almost one order of magnitude.

Keywords: Bonse-Hart technique, Ultra-Small-Angle Neutron Scattering .

1. INTRODUCTION

The characterization of hierarchical structures spanning a length scale from nanometers to microns is extremely important for materials research. Systems such as nano-composites of carbon blacks in polymers, protein hydro-gels, micro- and meso-porous materials, bones, and self-assembled fibril structures are all examples of complex systems whose microstructures cover length scales in the range of 10 angstroms to a few microns. Conventional SANS has proven important for providing structural information on length scales in the range of 10–1000 Å. The high penetration ability of neutrons, the magnetic moment, and unique contrast variation possibilities available through the use of isotope substitution make SANS an extremely powerful technique for the studies of bulk systems with complex hierarchical structures on these length scales. However, neutron techniques that can extend these capabilities to access length scales up to several microns are highly needed for materials research.

Recently, a Bonse-Hart-type Ultra-SANS (USANS) Double-Crystal Diffractometer (DCD) has been developed for neutron scattering at HFIR. In this instrument, the triple-bounce channel-cut Si monochromator and analyzer crystals were modified to prevent contamination of the rocking curve wings by single-bounce back-face reflections, end-face reflections and surface-induced scattering [1,2]. This breakthrough resulted in an improvement of the signal-to-noise ratio (SNR) by over three orders of magnitude. This new instrument has added nearly two orders of magnitude ($2 \cdot 10^{-5} \text{ \AA}^{-1} < Q < 10^{-3} \text{ \AA}^{-1}$, $Q = 4\pi \cdot \sin\theta/\lambda$, where 2θ is the scattering angle and λ is the neutron wavelength) to the range of length scales accessible to neutron scattering investigations and presently represents the state of the art for this class of instruments. Over twenty scientific groups from domestic and foreign institutions have used the ORNL USANS instrument, producing several significant scientific advances in petrology [3], polymer sciences [4], and geophysics [3-8]. One of the discoveries made using the HFIR USANS instrument was the observation of surface fractal structure of extremely long extent — over three orders of magnitude in the length scale — in sedimentary rocks [3]. This discovery was highlighted in Physical Review Letters Focus [5] and Science [6]. The instrument design concepts developed at ORNL have been applied subsequently in the development of new USANS instruments at NIST and in Europe and Japan. These developments demonstrate the significance and usefulness of this technique for broad application in structural studies of polymers, cements, colloids, complex liquids, rocks, clays and many other materials.

This technique is flux limited; hence, experiments require large samples and significant amounts of beam time even at high-flux reactors. There is presently a severe shortage of beam time available for USANS experiments for the scientific communities in polymers, biology, complex fluids, metallurgy, magnetic materials, physics and composites that needs to be addressed. It is expected that about 50% of the materials problems that SANS addresses in a wide range of scientific disciplines require data in the larger length scale region. This subset of problems can take advantage of the USANS technique. In addition, there

exist other systems that fundamentally require the USANS region for their characterization. Because SANS is one of the most heavily highly oversubscribed techniques at all user facilities worldwide, it is expected that a large scientific community already exists to use the USANS instruments. Thus, there is a real need for the development of high-throughput USANS instruments; this is possible only at high-intensity pulsed neutron sources such as SNS. Therefore, it is to be expected that further innovations in this field of neutron scattering instrumentation will be extremely useful to the general scientific community.

We are developing conceptual designs for Time-Of-Flight Ultra-Small Angle Neutron Scattering (TOF-USANS) instruments that allow the measurement of SANS data in the range of length scale from 1000 Å to 200 μm for the structural characterization of materials. We plan to build a prototype channel-cut double-crystal TOF-USANS instrument at the Argonne Intense Pulsed Neutron Source (IPNS) using the design concepts and characterize its performance with known systems. The ultimate goal of this work is to develop and test the design concepts necessary for the construction of advanced, powerful TOF-USANS instruments at SNS. These instruments represent a significant enhancement over their steady-state reactor-based counterparts through its ability to measure USANS data using time-of-flight (TOF) technique to separate and utilize multiple high-order harmonics of the Bragg reflected neutron flux. The latter allows significant enhancement in neutron flux as well as increase of the Q-resolution by almost one order of magnitude when compared to the corresponding single-wavelength reactor-based instruments. We considered two different configurations of the TOF-USANS camera: one optimized for the highest flux while preserving the conventional USANS Q-resolution and the other optimized for the highest Q-resolution while preserving flux.

2. BASIC CONCEPTS OF A TOF-USANS INSTRUMENT

This paper describes TOF-USANS instruments specifically designed to take advantage of the pulsed nature and high flux of the Spallation Neutron Source (SNS), particularly the high thermal neutron flux produced by the SNS water moderator with a poison depth of 25 mm. The novelty of this instrument is that neutrons with multiple harmonic wavelengths diffracted by the channel-cut monochromator/analyzer crystals set up at a given Bragg angle can be separated using TOF techniques. The time-of-flight information available due to the pulsed nature of the SNS allows the sorting of diffracted neutrons detecting not only by direction but also by energy or by wavelength. In Bragg diffraction from a single crystal, neutrons with a series of different wavelengths $\lambda_n = \lambda/n$ satisfying the Bragg relation, $n\lambda_n = 2d\sin\theta_B$, where d is the lattice spacing between a given set of crystal planes and $n = 1, 2, 3, \dots$ is the order of diffraction, are scattered at the same Bragg angle θ_B . Since the velocity of a neutron is inversely proportional to its wavelength, the corresponding diffraction peaks, $\lambda, \lambda/2, \lambda/3, \lambda/4$, etc., (see Fig. 1) can

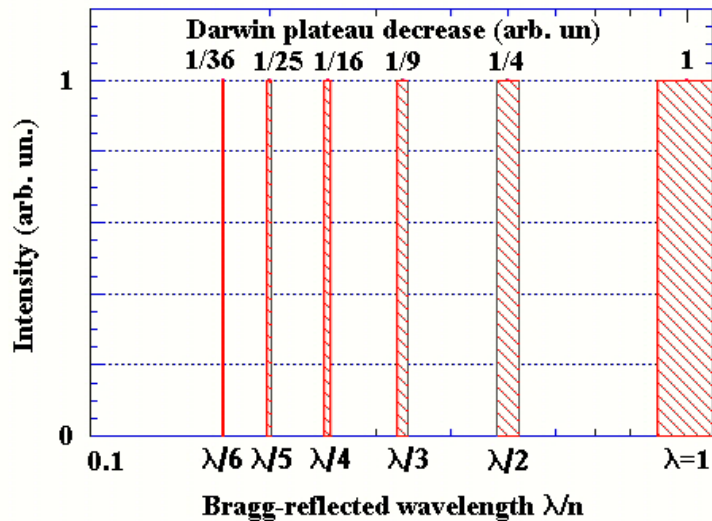


Fig. 1. Diffraction peaks Bragg-reflected from a perfect crystal oriented at a fixed angle with respect to the “white” primary beam or to the pre-monochromator made with the same crystal cut parallel to the same crystallographic plane.

be separated and detected independently using the TOF technique. This provides simultaneous parallel measurement of the USANS signal using up to, say, 8 different wavelengths, which leads to significant intensity enhancement compared to the monochromatic reactor-based USANS instruments while overcoming the problem of harmonic contamination. Moreover, since the angular resolution (the rocking curve width) of a DCD is proportional to λ_n^2 , the high order diffraction peaks, λ , $\lambda/2$, $\lambda/3$, $\lambda/4$, etc., allow the achievement of significantly higher Q-resolution.

According to the Darwin theory, changing the Bragg angle, θ_B can also vary the angular resolution. Because the reflectivity function of a perfect transparent crystal (valid for Si described here) to a first approximation has a rectangular shape, only one parameter, its Darwin Plateau (DP), $2\delta\theta_n$, is necessary for its characterization. This parameter is given by

$$2\delta\theta_n = [2|F(n)/\pi V_0] \cdot [(\lambda/n)^2/\sin 2\theta_B], \quad (1)$$

where V_0 is the volume of the crystallographic unit cell and $|F(n)|$ is the magnitude of the structure factor of Si, which is the same for all orders of the (220) reflection but oscillates with order n as $(1-\sin(\pi n/2))$ for the (111) family of reflections. The intensity reflected from a perfect crystal oriented at the Bragg angle within the Darwin plateau is usually very close to unity. This statement is valid not only for the first order reflection but also for its higher harmonics as shown in Fig. 1. It is worthwhile to note that the first term in formula (1) depends only on the parameters of a chosen crystal, thus the DP, $2\delta\theta(n)$, scales as $(\lambda/n)^2/\sin 2\theta_B$. Fig. 2 shows that the DP of the first order reflection calculated for Si(111) and Si(220) increases significantly in the range $20^\circ < \theta_B < 88^\circ$, as the Bragg angle is increased. Our conceptual designs for TOF-USANS instruments optimized for the highest flux and highest resolution are based on this ability to control the angular resolution and the wavelength of diffraction peaks, λ , $\lambda/2$, $\lambda/3$, $\lambda/4$, etc., by changing the Bragg angle and the d-spacing of the Si channel-cut crystals.

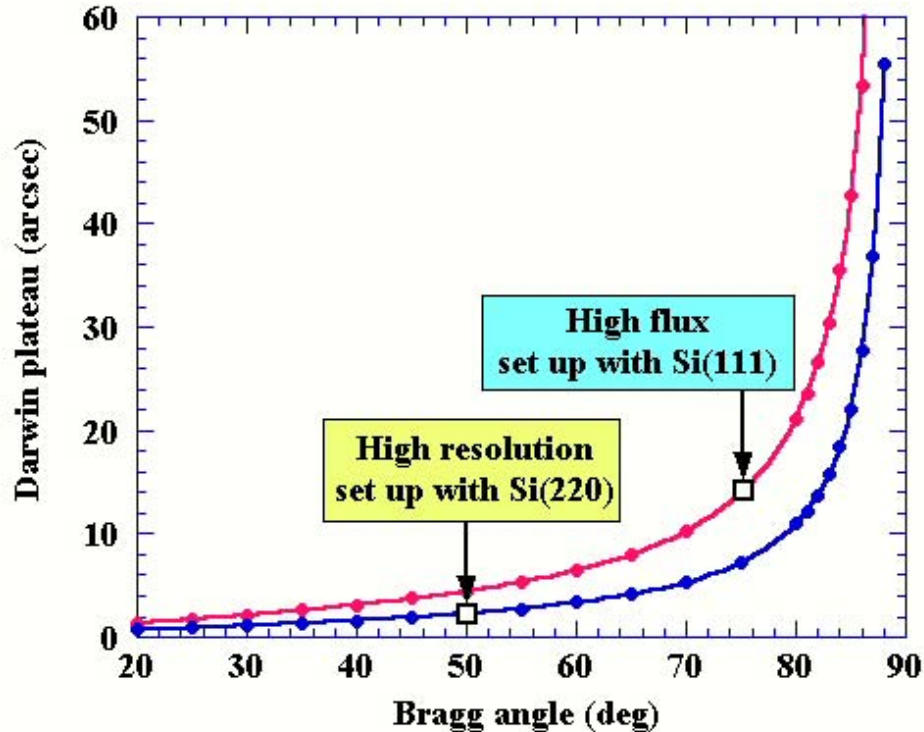


Fig. 2. Angular dependence of the Darwin plateau calculated for Si(111) and Si(220).

The scattering vector $Q = 4\pi\sin\theta/\lambda$ is the main parameter of any SANS experiment; its minimal value, Q_{\min} , determines the Q-resolution, ΔQ , for many types of the SANS instruments. The Bonse-Hart

TOF-USANS instrument is one such an instrument; ΔQ_n is conveniently connected to the value of Darwin plateau through the relation

$$\Delta Q_n = Q_{\min}(n) = 4\pi \sin[2\delta\theta_n]/\lambda_n \approx 8\pi\delta\theta_n/\lambda_n = [8F(n)/V_0] \cdot [(\lambda/n)/\sin 2\theta_B]. \quad (2)$$

Equation (2) clearly shows that $\Delta Q_n \sim \lambda/n$. Thus the resolution of a TOF-USANS instrument increases significantly when the high-order Bragg reflections are used.

3. TOF-USANS OPTIMIZED FOR THE HIGHEST FLUX

The SNS H₂O poisoned, decoupled moderator provides the highest flux of thermal neutrons in the range of wavelengths, $0.5 \text{ \AA} < \lambda < 2.0 \text{ \AA}$. Thus the optimal flux can be achieved by increasing density of the Bragg reflections in this range (see Fig.3). It is important to maintain $Q_{\min} \approx 2 \cdot 10^{-5} \text{ \AA}^{-1}$, which corresponds to Q-resolution of the reactor-based USANS instruments. Fig. 1 clearly indicates that the density of high-order Bragg reflections is increased with the increase of n. Therefore, the number of reflections in the range of wavelengths of interest, $0.5 \text{ \AA} < \lambda < 2.0 \text{ \AA}$, will be increased when the first order peak is shifted to higher values of λ . The latter, according to the Bragg formula, can be done by increasing θ_B , which also leads to the increase of DP (see Fig. 2). Fig. 4 shows a discrete spectrum of the neutron flux Bragg-reflected from

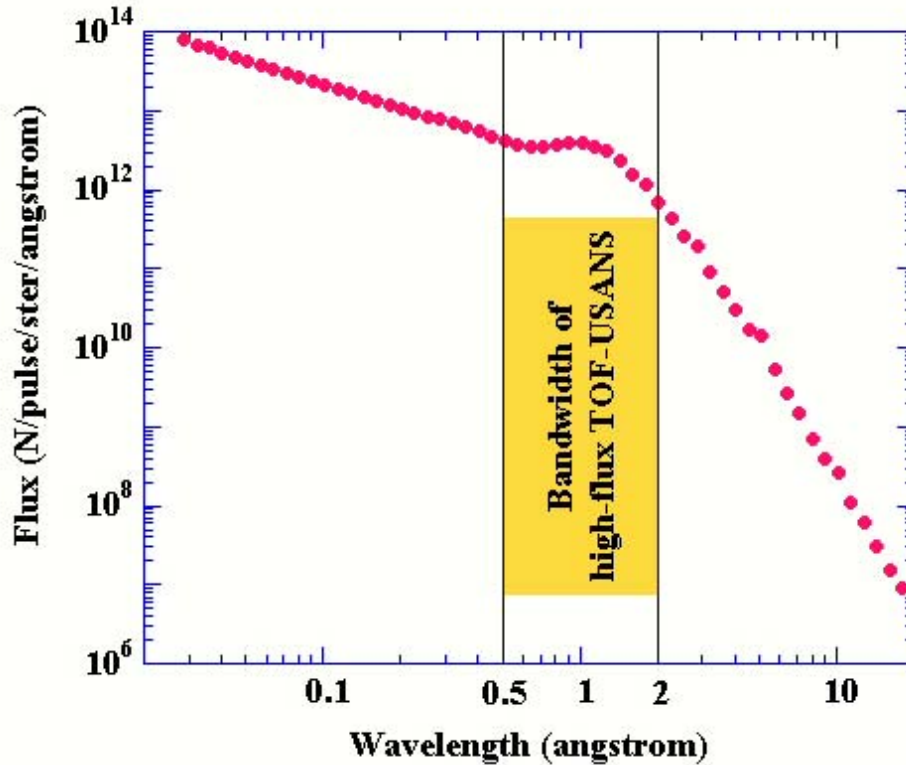


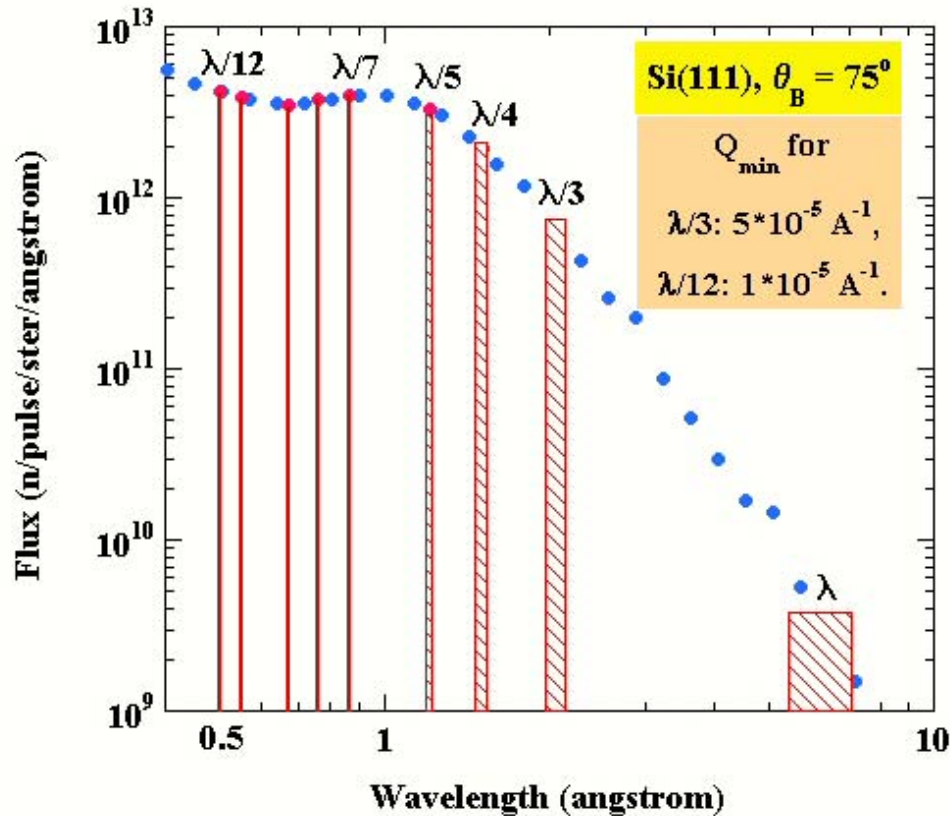
Fig. 3. Neutron flux originated by the SNS H₂O poisoned decoupled moderator and the bandwidth, $0.5 \text{ \AA} < \lambda < 2.0 \text{ \AA}$, chosen for the high-flux version of TOF-USANS.

the increase of DP (see Fig. 2). Fig. 4 shows a discrete spectrum of the neutron flux Bragg-reflected from a Si(111) crystal oriented at $\theta_B = 75^\circ$. The peaks, $\lambda, \lambda/3, \dots, \lambda/12$, are located in the range of wavelength, $0.2 \text{ \AA} < \lambda < 5 \text{ \AA}$, however, the first order reflection at $\lambda = 5.0 \text{ \AA}$ has relatively low peak intensity. Thus, in spite of a rather broad DP (~ 14 arcsec, see Table 1), its contribution to the total TOF-USANS flux summarized over all reflections shown in Fig. 4 seems to be insignificant. It is reasonable to abandon this peak as this decreases the upper cut-off of the operating bandwidth from $\lambda \approx 6.0 \text{ \AA}$ to $\lambda = 2.0 \text{ \AA}$ (see Fig. 3) and eliminates a possible time-frame overlapping problem almost without cost in either intensity or data quality. Thus, the high-flux USANS instrument based on triple-bounce Si(111) channel-cut crystals permits

Table 1. Bragg Diffraction Parameters for Si(111) and Si(220) useful for TOF-USANS.

Crystal, (h, k, l)	a, cell edge [Å]	d spacing [Å]	b_{coh} 10^{-12} cm	F, 10^{-4} [Å]	λ , opt. [Å]	θ_B opt. [deg]	Darwin width, $2\delta\theta$, [arcsec]	Missed orders
Si(111)	5.431	3.1355	0.415	2.316	6.057	75	13.931	$\lambda/2, \lambda/6, \lambda/10$
Si(220)	5.431	1.9201	0.415	3.203	2.942	50	2.3072	none

parallel measurements of 8 scattering curves per one angular scan using $\lambda/3$, $\lambda/4$, $\lambda/5$, $\lambda/7$, $\lambda/8$, $\lambda/9$, $\lambda/11$, $\lambda/12$ monochromatic lines (see Fig. 4). The Q-resolution of the TOF-USANS (see equation (3)) is higher for the high-order reflections because the Darwin plateau decreases as λ^2 , as shown qualitatively in Fig. 2. As a result one of the most important parameters, Q_{min} , varies from $Q_{\text{min}} \approx 5 \cdot 10^{-5} \text{ \AA}^{-1}$ for the $\lambda/3$

Fig. 4. Spectrum of Bragg reflections from Si(111) crystal set up at $\theta_B = 75^\circ$.

reflection to $Q_{\text{min}} \approx 1 \cdot 10^{-5} \text{ \AA}^{-1}$ for the $\lambda/12$ reflection. Therefore, the best Q-resolution of this setting is equal to or even slightly better than that of the corresponding reactor-based USANS cameras.

Fig. 4 gives us a qualitative picture of the high-order reflections but does not give clear information about the expected intensity gain. Fig. 5 shows a rough estimate of the gain in intensity that can be achieved at the TOF-USANS instrument compared to its reactor-based analogs. For this purpose, the intensity of each Bragg reflection is multiplied by $2\delta\theta(n)/[2\delta\theta(1) \approx 1.6 \text{ arcsec}]$, where the denominator corresponds to the Darwin plateau of the first-order Bragg reflection from Si(220) at the wavelength $\lambda = 2.4 \text{ \AA}$. This set of crystallographic parameters is chosen for the NIST USANS camera [9], and we have taken that as a reference reactor-based analog because we believe that the performance of this instrument is close to optimal. The total flux gain of the TOF-USANS camera can be estimated from the ratio $\{\Sigma I(\lambda(n)/n)\}/I(\lambda=2.4\text{\AA})$, where $\Sigma I(\lambda(n)/n)$ is the total normalized intensity of the all high-order reflections shown in Fig. 5 and $I(\lambda=2.4\text{\AA})$ is the intensity of the first order Bragg reflection from Si(220) at $\lambda=2.4\text{\AA}$,

which has the Darwin plateau, $2\delta\theta(1) \approx 1.6$ arcsec. This ratio gives a flux gain, ~ 18 , between a single-wavelength NIST USANS camera and a multi-wavelength TOF-USANS that we attribute to the enhanced performance of the instrument. The actual flux gain will be determined from the Monte-Carlo simulation of the SNS TOF-USANS instrument by taking into consideration of the source brightness and the optical

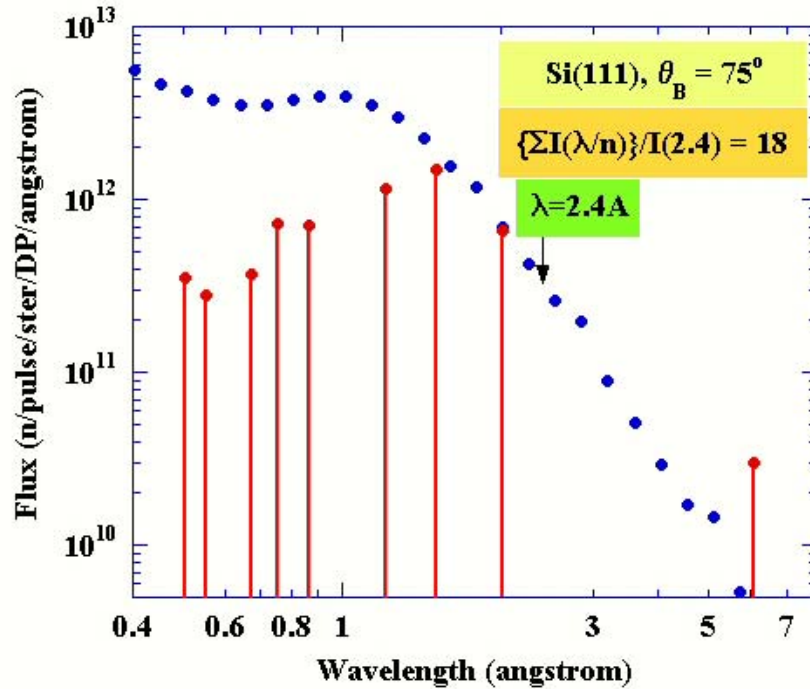


Fig. 5. Normalized spectrum of Bragg reflections from Si(111) crystal set up at $\theta_B = 75^\circ$.

components contribution.

Fig. 6 shows an optical scheme of the high-flux TOF-USANS camera with triple-bounce Si(111) channel-cut crystals (Fig. 7) designed for the Bragg angle $\theta_B = 75^\circ$. In this design the cross-section area at

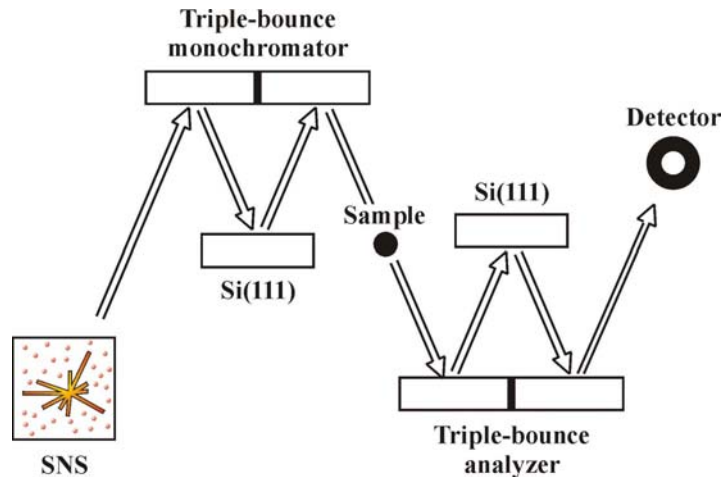


Fig. 6. Optical scheme of the high-flux TOF-USANS instrument with triple-bounce Si(111) crystals designed for the Bragg angle $\theta_B = 75^\circ$.

the sample position is as big as $50 \times 30 \text{ cm}^2$, which is similar to that for the NIST USANS camera. The layout in Fig. 6 does not include the upstream optical elements, a neutron guide and a pre-monochromator.

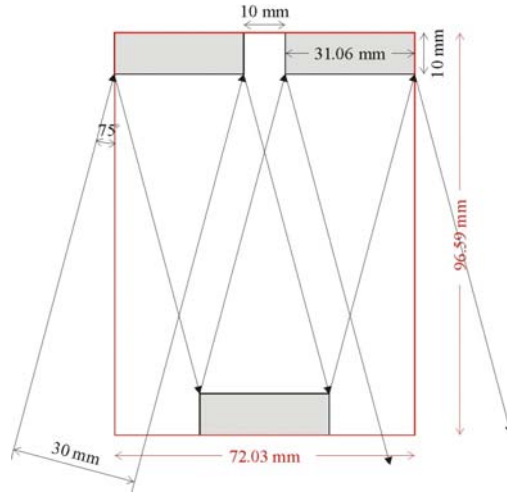


Fig. 7. Triple-bounce Si(111) channel-cut crystal designed for $\theta_B = 75^\circ$ and the horizontal size of neutron beam equal to 30 mm.

The triple-bounce Si(111) channel-cut crystal designed for $\theta_B = 75^\circ$ has two obvious advantages compared to the conventional channel-cut crystals with $\theta_B \leq 40^\circ$: First of all, contribution of the parasitic single-bounce back-face reflection (see [1, 2]) becomes smaller. Secondly, the surface-induced scattering [2] also must be significantly weaker when the Bragg angle is increased.

3. TOF-USANS OPTIMIZED FOR THE HIGHEST RESOLUTION

The high-resolution TOF-USANS instrument is also optimized for the same SNS H_2O poisoned decoupled moderator choosing Si(220) crystal set up at the Bragg angle, $\theta_B = 50^\circ$. This configuration allows usage of 6 Bragg peaks (see Fig. 8) in the wavelength range, $0.49 \text{ \AA} < \lambda < 3 \text{ \AA}$, with the best value

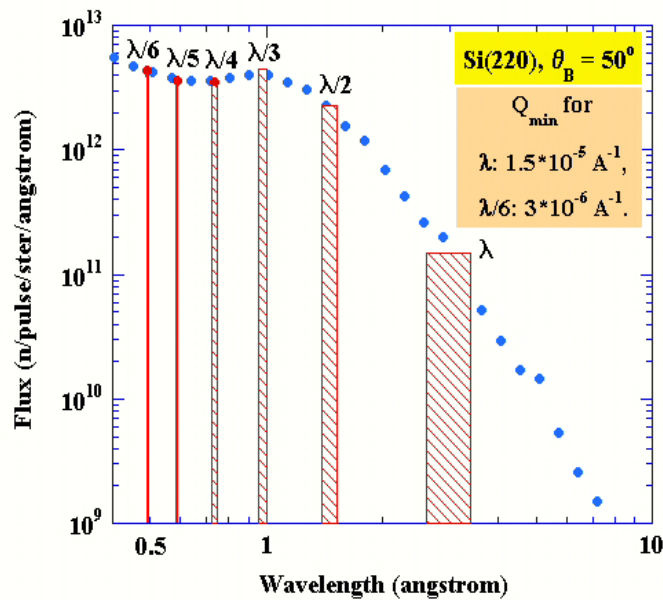


Fig. 8. Spectrum of Bragg reflections from Si(220) crystal set up at $\theta_B = 50^\circ$.

of $Q_{\min} = 2.5 \cdot 10^{-6} \text{ \AA}^{-1}$. This Q-resolution is almost one order of magnitude higher than that for the best present reactor-based Bonse-Hart USANS instruments. The main crystallographic and diffraction parameters for these two configurations of the TOF-USANS are shown in Table 1.

The total intensity gain for this configuration is calculated similarly to that made for the high-flux TOF-USANS. This gain factor of 7 estimated by the same way (see Fig. 9), is about 2.2 times smaller than that for the high-flux TOF-USANS; however it's still significant. Fig. 10 and 11 demonstrate the corresponding changes in the optical scheme and in the channel-cut crystal design.

The two TOF-USANS instruments described here represent a novel approach to extending the range and usefulness of the Bonse-Hart USANS technique. These instruments will provide the SNS and other pulsed neutron sources with a way to build world-class USANS instruments. These instruments will be a valuable and exciting complement to the suite of instruments already planned, extending the capabilities of the SNS in new directions.

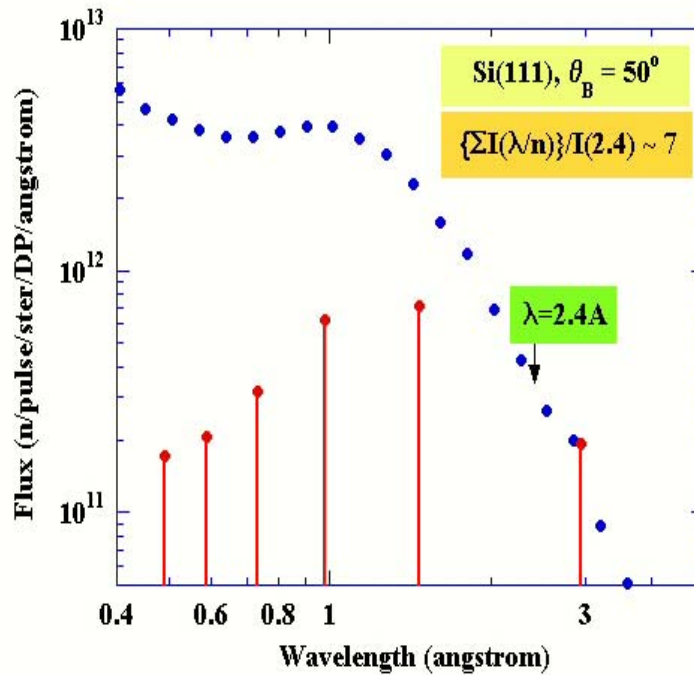


Fig. 9. Normalized spectrum of Bragg reflections from Si(111) crystal set up at $\theta_B = 50^\circ$.

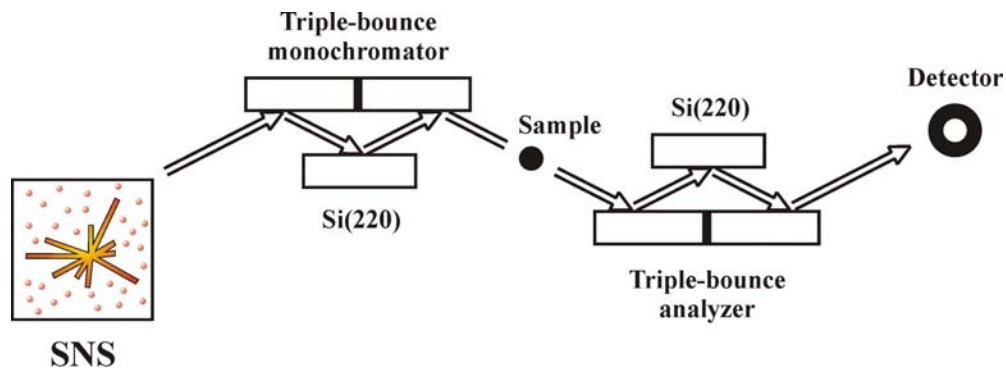


Fig. 10. Optical scheme of the high-resolution TOF-USANS instrument with triple-bounce Si(220) crystals designed for the Bragg angle, $\theta_B = 50^\circ$.

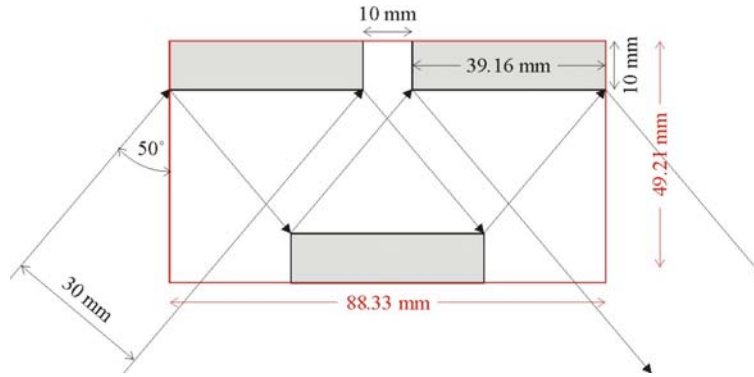


Fig. 11. Triple-bounce Si(220) channel-cut crystal designed for $\theta_B = 50^\circ$ and the horizontal size of neutron beam equal to 30 mm.

4. SUMMARY

The present calculations clearly show the following advantages of the multi-order TOF-USANS instrument:

- the flux gain factor related to this innovative multi-wavelength performance is ~ 18 for the high-flux set up and ~ 7 for the high-resolution version of the instrument.
- the high-resolution set up dramatically extends the value of Q_{\min} , from $2 \cdot 10^{-5} \text{ \AA}^{-1}$ to $\sim 3 \cdot 10^{-6} \text{ \AA}^{-1}$, which will allow measurements of enormously large inhomogeneities with dimensions up to 200 μm .
- parallel measurements at different wavelengths will be very helpful for diagnosing multiple scattering in the USANS experiments, which is very common for this dynamical range of neutron diffraction.
- the increased Bragg angle of the triple-bounce channel-cut Si crystals, $\theta_B = 50^\circ$ and $\theta_B = 75^\circ$, will lead to further reduction in parasitic scattering that includes contribution from the back-face reflection and the surface-induced scattering, and as a result to the further increase of the signal-to-noise ratio.

5. REFERENCES

1. M. Agamalian, G.D. Wignall & R. Triolo, *J. Appl. Cryst.*, **30**, 345-352, (1997).
2. M. Agamalian, D.K. Christen, A.R. Drews, C.J. Glinka, H. Matsuoka & G.D. Wignall, *J. Appl. Cryst.*, **31**, 235-240, (1998).
3. A.P. Radlinski, E.Z. Radlinska, M. Agamalian, G.D. Wignall, P. Lindner and O.G. Randl, *Phys. Rev. Lett.*, **82**, 3078-3081, (1999).
4. M. Agamalian, R.G. Alamo, J.D. Londono, L. Mandelkern, and G.D. Wignall. *J. Appl. Cryst.*, **33**, 843-846, (2000).
5. <http://focus.aps.org/v3/st22.html>
6. <http://www.academicpress.com/inscight/04191999/grapha.htm>
7. http://www.pnl.gov/er_news/10_96/briefly.htm#ornl
8. Researcher upgrades ORNL neutron scattering facility, p. 8, DOE This Month, April, 1999.
9. Perfect Crystal Diffractometer (PCD) for Ultra-High Resolution Small-Angle Neutron Scattering, <http://www.ncnr.nist.gov/instruments/usans>